Maximum Surface Albedo of Seasonally Snow-Covered Lands in the Northern Hemisphere

DAVID A. ROBINSON AND GEORGE KUKLA

Lamont-Doherty Geological Observatory of Columbia University, Palisades, NY 10964

(Manuscript received 15 May 1984, in final form 20 November 1984)

ABSTRACT

Areally weighted clear sky surface albedo of snow-covered land in the middle and high latitudes of the Northern Hemisphere was measured from satellite imagery in 1 × 1° latitude–longitude cells. The study area included 87% of the land polewards of 25°N, where Dickson and Posey found the probability of the seasonal occurrence of snow cover over 2.5 cm deep to be greater than zero. Albedo is 0.60 in Eurasia and 0.56 in North America, approximately 3.5 times greater than snow-free conditions. The highest average value for a 5° latitudinal zone is 0.77 at 70–75°N. The lowest is 0.43 at 60–65°N, which includes 0.36 in Eurasia and 0.58 in North America. The low albedo is due to the masking of snow covered ground by the canopy of coniferous forests.

Data were obtained by image processor analyses of Defense Meteorological Satellite Program imagery. Scene brightness was converted to surface albedo by linear interpolation between bright and dark snow-covered surfaces with known albedo.

The resulting chart is a refinement of an earlier product. The 1 × 1° digital data set is available for use in climate modeling.

1. Introduction

The albedo of the earth's surface plays an important role in the earth–atmosphere energy budget (Namias, 1962; Rockwood and Cox, 1978; Ramanathan *et al.*, 1979). The ratio of solar energy absorbed by the surface to that by the atmosphere is close to 2.5:1. With the exception of sea ice, land surfaces show the largest annual and interannual variation in albedo, largely due to seasonal snow cover (Bauer and Dutton, 1962; Robock, 1980).

The albedo of snow-covered lands varies considerably, as a function of the type and density of vegetative cover, age and depth of snow, etc. Local and regional studies have documented this variability (e.g Kung *et al.*, 1964; McFadden and Ragotzkie, 1967; Lillesand *et al.*, 1982; Jurik and Gates, 1983; Robinson *et al.*, 1983). On a hemispheric scale, several researchers have attempted to reconstruct the albedo of snow-covered lands. They have used data on the distribution of vegetation as charted in atlases, assigning each surface type an albedo based on parameterized values (Posey and Clapp, 1964; Hummel and Reck, 1979; Robock, 1980). Others have used satellite data to estimate the albedo of snow-covered zones over a specified interval (Preuss and Geleyn, 1980; Kukla and Robinson, 1980). Here we report results of a different approach. We measured the maximum surface albedo of land covered with seasonal snow in 1 × 1° latitude–longitude cells over the Northern Hemisphere in selected clear sky scenes of Defense Meteorological Satellite program (DMSP) imagery. Film density, which is in linear proportion to the satellite image brightness (Fett and Bohan, 1977), was measured on an image processor. Surface albedo was determined by assuming a linear relationship between brightness and albedo.

We selected scenes within images with stabilized deep snow cover because they provide an upper limit to albedo parameterizations used in climate models and because snow cover exerts its maximum impact on climate when it is fresh and relatively deep. Albedo of shallower or partly dissipated older snow can be obtained through interpolation between snow-free and full snow cover values.

Land potentially covered by seasonal snow was delimited as the region north of Dickson and Posey's (1967) line with 0% probability of having at least 2.5 cm of snow on the ground at the end of January or February, whichever reaches farther south (Fig. 1). The area includes 60% of all Northern Hemisphere land and 87% of the land north of 25°N.

2. Data Sources

A complete description of the DMSP satellite and imagery used in our analysis is found in Fett and Bohan (1977). The polar orbiting satellite crosses the equator at noon. It is equipped with an Operational Line Scan System sensor (OLS) with a nadir resolution of 2.8 km. The OLS provides near-constant image

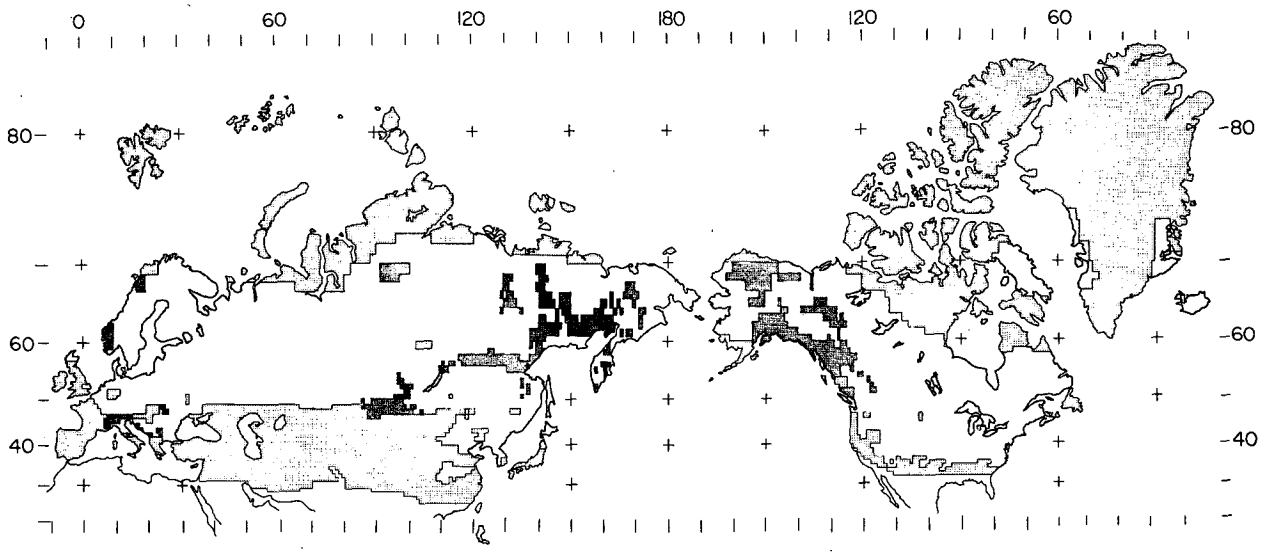

FIG. 1. Northern Hemisphere land with a potential of developing seasonal snow cover. Scene brightness was measured on an image processor for each 1 × 1° cell shown with moderate stipple. Cells where brightness was adjusted downwards in the mountains are dark stippled and regions where albedo was inferred, light stippled. (Over arctic tundra, 50 cells, shown as inferred, were measured at random.)

resolution with optical compensation for motion across the 3000 km scan tract. Bidirectional reflectance of the earth–atmosphere system is recorded and normalized for solar illumination. Gain changes are smooth except at low solar elevations. Sensor saturation is not a problem over snow-covered regions (Bunting and d'Entremont, 1982).

The spectral range of the DMSP sensor is between 0.4 and 1.1 μm, where the majority of solar radiation reaching the surface is found (Male and Granger, 1981). This provides a more balanced view of surface brightness than that gathered by narrow-band single-channel sensors. The peak sensitivity is at 0.8 μm, in the near-infrared (NIR) spectral region where snow reflectivity begins to fall and vegetation reflectivity rises appreciably. Bryazgin and Koptev (1970) measured surface reflectivities of dry, moist and wet snow in the 0.4–1.0 μm range. Their results are close to the full shortwave (0.28–2.8 μm) albedos measured by others (eg. Maykut and Church, 1973; Carroll and Fitch, 1981; Robinson and Kukla, 1984). Thus, no spectral band correction was deemed necessary to transform the values of the DMSP sensor to full spectrum albedos. The sensor spectral range is also excellent for the discrimination of clouds and fog, due to its extension into the NIR where these features are more easily recognized (Fett and Isaacs, 1979).

Daily DMSP imagery is available in Transverse Mercator projection on ungridded positive film transparencies scaled at 1:15 × 10^6. The processed film density is linearly proportional to scene reflectivity. Digital data are not archived and are unavailable.

A scene within an image was chosen for measurement when the following specifications were met:

1) Snow was on the ground.

2) Skies were clear. (High cirrus and subresolution clouds were eliminated by comparing the surface contrast in noon images on consecutive days.)

3) The solar zenith angle (SZA) at the time of the noon satellite overpass was between 60 and 70°. This criterion was chosen to equalize potential specular and shading effects and to minimize brightness deviations stemming from different illumination.

4) Scenes were within the middle half of an imaged swath. This was done to minimize the effect of oblique scan angles and maximize ground resolution, which decreases from 2.5 km at nadir to 3.5 km halfway towards the margins of an image.

5) Transparency quality was good. Images which were poorly developed or had pronounced vertical banding were eliminated.

6) A scene exhibited maximum surface brightness.

a. Selection of scenes with maximum surface brightness

The first step required in determining whether maximum surface brightness was being exhibited was to recognize whether snow cover was present. The keys to snow recognition were pattern continuity, landmark identification and texture revealed by variations in surface brightness (Wark *et al.*, 1962; Conover, 1965).

The surface brightness of a snow covered area is a function of the type and density of vegetation and the depth and age of the snow. As the vegetation remains relatively constant from winter to winter, snow depth and age are primarily responsible for

brightness variability over an area. Brightness increases rapidly with snow depth, regardless of age (Kung *et al.*, 1964; Barnes and Bowley, 1968; McGinnis *et al.*, 1975; Lillesand *et al.*, 1982; Robinson and Kukla, 1982). Once the depth reaches approximately 15 cm, further increase in reflectivity with depth is slow. The age and state of the snow surface, not depth, become the critical variables affecting surface brightness.

A typical DMSP scene covering most of western Asia is shown in Fig. 2. The snow line in the open steppe is relatively sharp (A–B). The major difficulty in recognizing the snow in this zone results from cloud cover (C). The snow is patchy towards the east (D). Distinctive brightness textures north of the snowline are due to different densities of vegetation (E, F, G). They are site-specific and can be used as a characteristic brightness signature of a given locality. Surface albedo would be overestimated in regions with dense vegetation were cloud cover not recognized. Snow covered lakes, rivers and forest openings help in determining the presence of snow in forested zones (H).

Multiple scenes of a region taken over a several-day interval were compared in order to determine whether the area was exhibiting maximum brightness. If the texture and contrast remained stable for several days it was concluded that a relatively deep dry snow cover was present. Comparisons over longer intervals

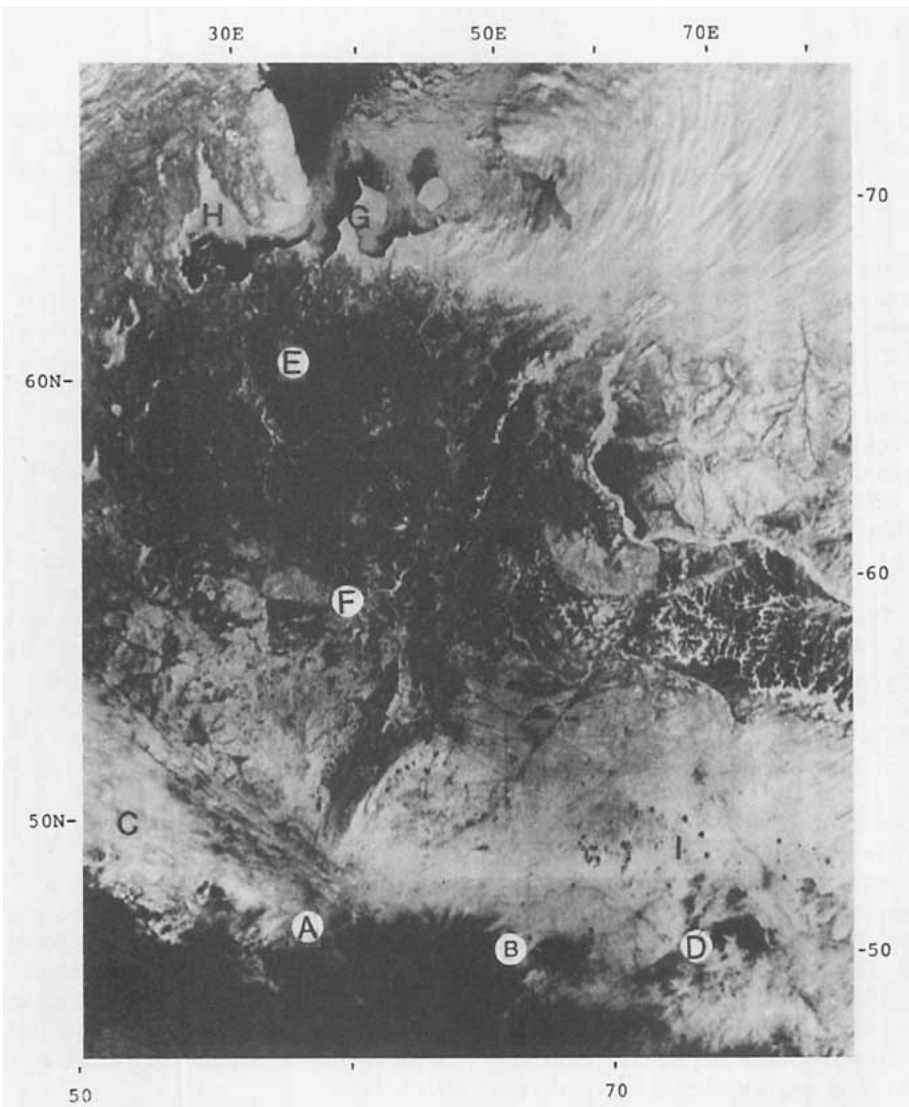

FIG. 2. A portion of a DMSP image covering northeast Europe and west Asia on 8 April 1979. Observed features include the snowline cutting through the central Asian steppe (A–B), cloud cover (C), patchy snow cover (D), fully snow covered regions with different densities of vegetation (E–G) and snow covered frozen water bodies (H). The region seen in Fig. 3 is marked with an I.

also helped in the decision process. For instance, in Fig. 3 the Siberian steppe is recognized on 23 March 1979 as being only partially snow covered by comparing it with the 19 February 1979 scene (Fig. 3a). The lightly vegetated swamp (point 1) is much darker on 23 March, as are areas to the southeast (point 2). The dark pattern of roads and rails radiating from darker cities (point 3) is also more pronounced on 23 March. Standard deviation, skewness and kurtosis of the brightness field analysed on the image processor were also used as indicators of snow cover stability (Robinson and Kukla, 1982).

We also examined published ground truth data on snow depth or snowfalls on or close to the scene date. These included U.S. Air Force charts of Northern Hemisphere snow depth and age (Woronicz, 1981), Canadian data from *Climatic Perspectives* (Atmospheric Environment Services, 1978–84) and U.S.

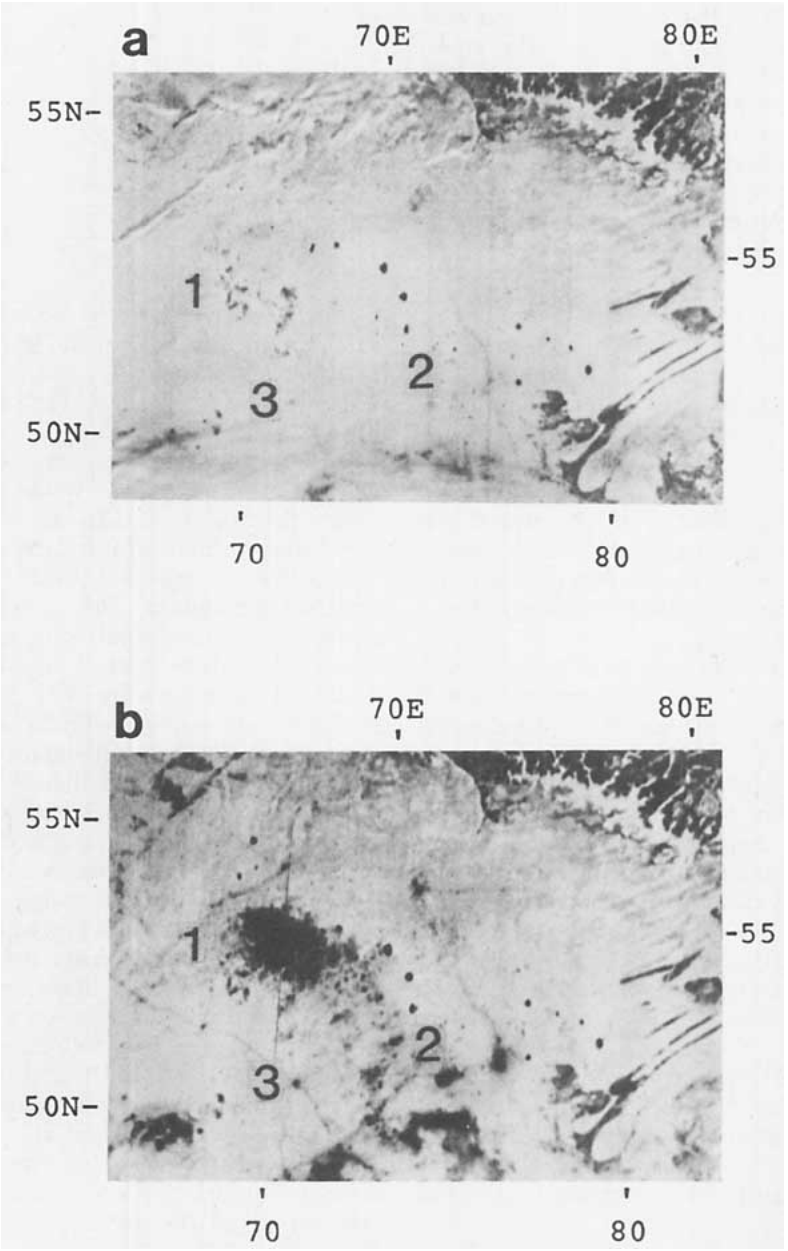

FIG. 3. A portion of DMSP image covering Asian steppe on 19 February 1979 (a) and 23 March 1979 (b). Brightness between the two images differs over the lightly vegetated swamp (1), clear areas to the southeast of the swamp (2) and in and around cities (3). On 23 March the swamp was covered by less extensive snow than on 8 April (cf. Fig. 2, region I); however, the snow cover was more complete along the southern portion of this region on 23 March.

information from the *Weekly Weather and Crop Bulletin* (U.S. Department of Commerce, 1914–) and *Climatological Data* (U.S. Department of Commerce, 1978–79). Finally, reports on average snow depth, duration and stability over the USSR (Kopanev, 1976a,b, 1978; Kurilova *et al.*, 1976) and Canada (Potter, 1965; Goodison, 1981) were examined.

Although the age of the snow surface could not be reliably established, it is expected that either fresh or blowing snow was deposited over most areas no more than several days before the date of the analyzed image. Brightness was measured only if the above tests indicated the presence of at least 15 cm deep dry snow. Snow or hoarfrost sticking to tree branches can considerably increase regional albedo. However, with clear skies such features do not last long and were considered to have a negligible impact on both regional albedo and our measurements.

TABLE 1. Correlation coefficients of duplicate measurements of cell brightness. In A the brightness of individual 1 × 1° cells was twice independently measured on the same image using identical standardization techniques. Results from 46 to 86 cells in each test scene were plotted and the correlation coefficients calculated. In B a similar procedure was followed, except that the brightness of a test cell was compared in images taken one or two days apart.

Number of cells	Correlation coefficient
A	
86	0.98
46	0.99
76	0.99
B	
86	0.96
86	0.98
86	0.98
71	0.99

b. Analysis

The DMSP imagery was analyzed on an image processor, which treated a projected portion of an image as 307 000 discrete pixels, assigning each a gray scale value from black (0) to white (255). Measured scenes within a projected image which met the study criteria ranged in size from approximately 62 000 to 160 000 km^2 and included 10 000 to 250 000 pixels. Output consisted of a brightness histogram, average brightness, standard deviation, skewness and kurtosis. Projected scenes were gridded into 1 × 1° cells by locating surface landmarks in a detailed atlas (Shurov, 1954).

The 109 scenes measured consisted of snow covered tundra, different types of forest and farmland as well as wasteland and semidesert. Scenes were measured from 75 images in 1979 and 5 in 1978. To assure continuity of the brightness scale, a newly measured scene had to overlap previously measured ones. Brightness of the overlapping scenes was then equalized by aperture adjustment of the processor lens. All scenes were identically calibrated. This procedure was tested by comparing the brightness of a single cell twice measured independently. In another test, the same cell was measured in clear sky scenes taken one or two days apart (Table 1). High correlations were found in both tests.

Since the interior of snow covered polar tundra is uniformly bright, only 50 cells were measured at random and the resulting average applied to the remainder. Water bodies smaller than 1 × 1° were included in the measurements, whereas larger ones were not.

Scene brightness was converted to surface albedo through a linear interpolation between the brightest arctic tundra and darkest snow covered forest, which were assigned parameterized albedos of 0.80 and 0.18, respectively. These corresponded to brightness values of 30 and 140, respectively. Parameterized regional surface albedos of the two standard surfaces were derived from published clear-sky measurements (eg. Jackson, 1961; Kung *et al.*, 1964; Federer, 1968; O'Neill and Gray, 1973; Robinson *et al.*, 1983). Surface albedos under cloudy skies may be as much as 0.10 greater over open snow fields (Grenfell and Maykut, 1977; Petzold, 1977; Carroll and Fitch, 1981). Brightness as high as the tundra was also found over portions of farmland and semidesert, but in the 1 × 1° cells only wide open farmland approached the tundra. The darkest value in a snow covered zone corresponds to a predominantly coniferous forest where most of the snow covered ground is masked by the canopy (cf. Fig. 2). No 1 × 1° cell averaged such a low brightness. On a subresolution scale, the albedo of a fully snow-covered coniferous forest may be even lower than 0.18. However, at the resolution of the imagery, some snow is almost always exposed in windfall gaps of the canopy, in stands of deciduous trees or on frozen water bodies. Shine and Henderson-Sellers (1983), using a radiative transfer scheme, showed that this procedure is justified when using DMSP imagery. Preuss and Geleyn (1980) also showed that there is a linear relationship between clear-sky planetary and surface albedo.

Brightness values over 140, exceeding the maximum tundra value, were only found over high elevations in Greenland and in mountainous regions. In both cases albedo was truncated at 0.80. The reason for the high brightness is the low atmospheric attenuation at high altitudes and enhanced reflection from sun oriented slopes (Dozier and Frew, 1981; Dave and Bernstein, 1982). The truncation amounted to a reduction of no more than 0.03 in the average albedo of any 1 × 1° mountainous cell from the measured value and occurred in less than 5% of the measured blocks. Figure 1 shows the cells in which a reduction was applied. No other efforts were made to account

for brightness variations resulting from scene geometry.

In 1979 the winter snow cover over the Northern Hemisphere was extensive and the quality of the DMSP imagery was good. There were, however, regions that remained snowfree or were never covered to a sufficient depth. Imagery from the winter of 1978 was then checked. Following this, some zones were still unavailable for measurement within the area that potentially develops a seasonal snow cover (cf. Fig. 1). Most were located in arid and semiarid areas of southern Asia (Ginsburg *et al.*, 1970), where albedo inference is simplified by the general absence of tall or dense vegetation (Wiebecke, 1971; Ni *et al.*, 1975; Olson and Watts, 1982; Matthews, 1983) protruding through the snow. Albedo for such cells was inferred from 1) brightness measured in partially snow-covered DMSP images; 2) comparisons of brightness values of fully and partially snow-covered areas elsewhere, as shown in NOAA polar orbiting Very High Resolution Radiometer (VHRR), Advanced VHRR and Geostationary Operational Environmental Satellite imagery; 3) comparisons with analogous surface types and terrains under full snow cover; 4) vegetation charts and atlases; (Wiebecke, 1971; Olson and Watts, 1982) and 5) Landsat mosaics of China and adjacent regions (Ni *et al.*, 1975) and the United States (U.S. Dept. of Agriculture, 1974; National Geographic Society, 1976).

The reported albedo of a measured cell may be up to 0.10 too low or 0.05 too high. This uncertainty can only be roughly estimated, as no data set on a similar scale is available for comparison. The principal sources of potential error lie in 1) the choice of albedo for the bright and dark calibration fields and 2) measurements being made over unrecognized shallow or melting snow. The albedo of a snow-free coniferous forest is close to 0.13 (eg. Kung *et al.*, 1964; Federer, 1968); this gives the maximum downward error of our calibration scale. Albedos as high as 0.90 were only reported over glaciers in polar regions and at high solar zenith angles (eg. Maykut and Church, 1973; Carroll and Fitch, 1981). They represent our upward error bracket. Aged snow fields when wet may be more than 0.10 lower than when fresh and dry (eg. McFadden and Ragotski, 1967; Grenfell *et al.*, 1981); however, melting snow is usually located in the vicinity of the snow line and associated with patchy snow fields. Where stable continuous snow in the interior of the pack is wet, granular and/or glazed its albedo is generally higher than 0.70.

Uncertainties in cells where albedo was inferred are estimated to be ±0.10, since in most such cells tall vegetation, which would make inferences considerably less accurate, is lacking.

Our satellite-derived results agree well with the albedo of a cell located between 41–42°N and 74–75°W computed from a model based on aerially determined albedos of individual surface types, whose areal distribution was derived from a land use census (Robinson, 1984). The maximum model albedo in the cell is 0.44, while the satellite-derived value is 0.42.

Potential errors due to the spectral limitations of the OLS are considered minor, based on the previously discussed measurements of Bryazgin and Koptev (1970) and the theoretical study of Shine and Henderson-Sellers (1983). Errors due to the bidirectional nature of the satellite measurements are also assumed minor, based on a satellite study of the angular dependence of reflected radiation by Taylor and Stowe (1984). Their study showed signals close to isotropic from snow covers observed at solar zenith angles and DMSP scan angles chosen in our study.

3. Results

Maximum estimated surface albedo over Northern Hemisphere lands with the potential of developing a seasonal snow cover is shown in Fig. 4. Values are stepped in 0.10 increments. Data for each 1 × 1° cell is available on tape at Lamont.

The correlation between the albedo of snow-covered surfaces and image brightness is seen by comparing the west Asian portion of Fig. 4 with Fig. 2. Full snow cover is generally 5° or more to the north of the snow line. Figure 2 contains cells having the lowest (E) and the highest (G) albedos measured in this study: 0.21 and 0.80, respectively. Polar tundra has an albedo close to 0.80, while open farmland and steppe show values 0.05–0.10 lower.

A broad zonal distribution of vegetation is apparent in Fig. 4. This is particularly clear in Asia, where the albedo rises from 0.36 over the boreal forests at 60–65°N to 0.76 over the tundra farther north (Table 2). The largest intercontinental range was found in the 60–65°N belt, where the average albedo is 0.58 in North America. This high value is due to the soutward extension of bright polar tundra into northeastern Canada.

Figure 5 shows the zonal distribution of albedo in two 20° wide meridional swaths, one in east Asia, the other in central North America. The latter runs southward from the homogeneously bright tundra of the Canadian archipelago and Keewatin district through the northwest-trending lake-dotted boreal forest to the prairie and farmland of south central Canada and the central United States. The Asian swath contains a wide forested zone cut by the brighter Yablonov and Stanov mountain ranges between 54 and 59°. Tundra and farmland lie, respectively, to the north and south of the forests.

Coastal forests in the middle latitudes result in lower winter albedos in these areas of abundant moisture than in the middle of the continents. In the

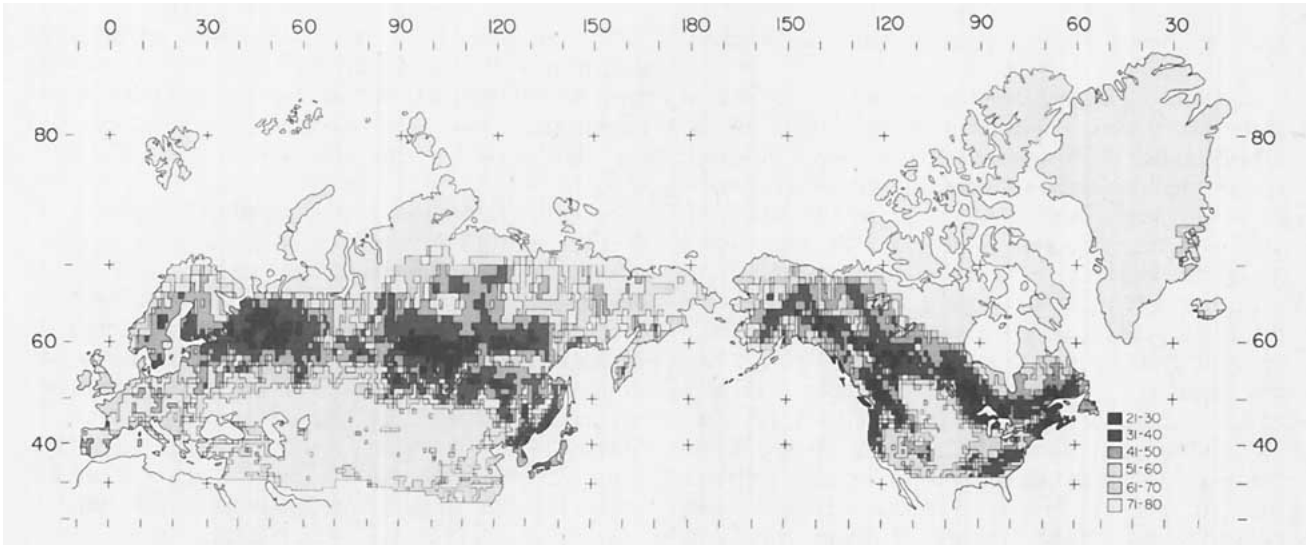

FIG. 4. Maximum surface albedo over Northern Hemisphere land with the potential of developing seasonal snow cover. Cells, measuring 1 × 1°, are marked in 0.10 increments. Comparisons with cloud-free portions of Fig. 2 may be made in the region 60–70°N, 30–75°E. All measurement criteria are met in this portion of Fig. 2, with the exception of the SZA, which is too low south of 67°.

past this would have been more evident. However, in the past centuries man has deforested large portions of Europe, eastern China and the eastern United States (Matthews, 1983). This has raised the winter albedo in the originally forested zones by about 0.30 (Robinson, 1984).

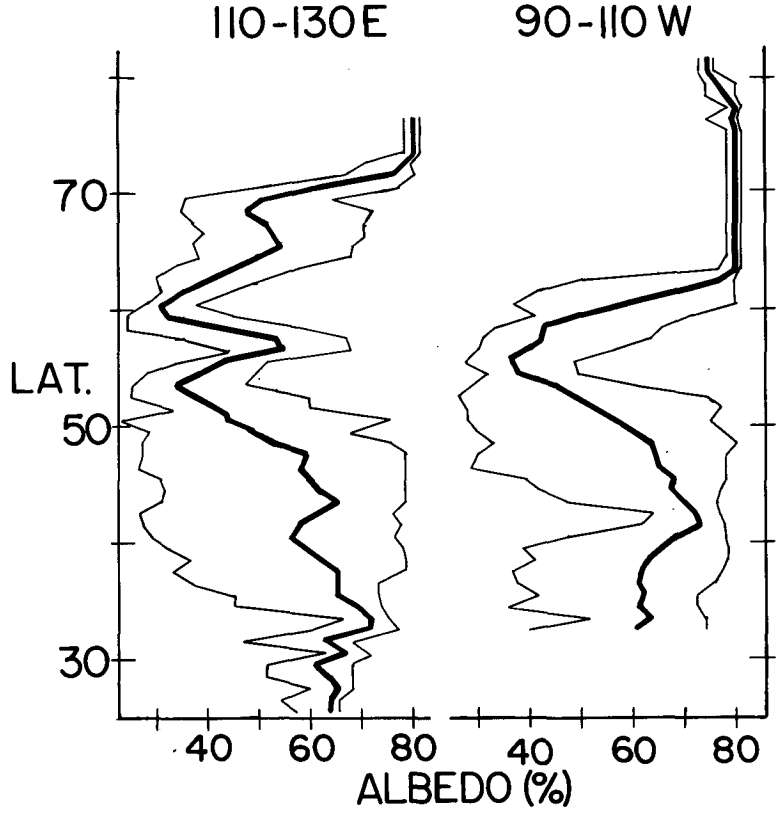

FIG. 5. Maximum surface albedo of seasonally snow covered lands in 1° latitudinal steps averaged across two 20° wide longitudinal swaths (heavy lines). The range in albedo for the 20 cells in each latitudinal zone is shown with thin lines.

Mean albedos over the snow-covered Eurasian (0.60) and North American (0.56) continents are approximately three to four times higher than their snow-free values (Posey and Clapp, 1964; Hummel and Reck, 1979; Kukla and Robinson, 1980) (Table 2). The addition of Greenland raises the hemispheric mean albedo by less than 0.01.

4. Discussion

Others have estimated surface albedo by calibrating satellite brightness with ground truth of portions of an imaged scene. Richardson (1982) summarizes applications of this technique to Landsat imagery. More recently, Landsat data were used by Kowalik *et al.* (1982) and Mekler and Joseph (1983). Data from the Skylab S-192 Scanner System was similarly successfully employed to estimate surface albedos (Barnes and Bowley, 1977; Pease *et al.*, 1980), as was Applications Technology Satellite data (Norton *et al.*, 1979) and Synchronous Meteorological Satellite data (Rockwood and Cox, 1978). Several studies assume a linear relationship between digital counts and reflectivity. These include ones using Heat Capacity Mapping Mission data (Vukovich, 1983; Gurney and Hall, 1983), NOAA VHRR results (Henderson-Sellers, 1980) and Russian satellites (Kondratyev *et al.*, 1974). All of the preceding studies were regional in scale. Only Gurney and Hall considered a snow-covered region.

In addition to being time and cost effective, albedo determinations from DMSP satellite imagery benefit from its broad spatial coverage, linear density processing, wide spectral range and lack of saturation problems. While the satellite limitations are not negligible, they are minor compared to the dramatic variability of surface brightness on short time scales caused by the presence of snow.

The present product, which we will refer to in the following discussion as "Max", is an improved version of an earlier one (Kukla and Robinson, 1981). The first was based on a visual examination of imagery from a variety of satellites. Clear-sky brightness was segregated into six classes and a parameterized albedo was assigned to each. There is a reasonable agreement between the two products, but the earlier chart is less detailed and brightness standards were not as rigidly maintained.

No earlier studies were meant to represent maximum surface albedo, although snow-covered continental interiors may be considered as charted at or close to maximum values. The North American clear-sky albedos of Kung *et al.* (1964) north of their 5 inch snowline are mostly 0.10 above Max. Over southeastern Canada and the northeastern United States the values agree. Over extreme south central Canada and the central United States the Max values are higher. Boundaries of sharply different albedos are similar in both products. Posey and Clapp (1964) differ from Max by less than 0.10 over forested regions of North America and central Siberia. Polar tundra and most of Quebec have values 0.10 lower than Max. Posey and Clapp's forest values are approximately 0.20 higher over northwestern USSR and 0.20 lower in eastern Siberia. Only the most general comparisons can be drawn between Max results and those of Hummel and Reck (1979) and Kondratyev *et al.* (1982). Forest albedos are higher than Max in each, by over 0.20 in some regions; particularly so in the latter product. A closer agreement is reached in the higher latitudes. There may exist a difference between the clear sky surface albedos as defined in Max and the albedos reported in the latter three studies due to the possible incorporation of clear and cloudy sky albedos into their parameterizations. However, as most published ground truth winter albedos were measured under clear skies (Robinson, 1984), it is doubtful that this can fully explain the differences noted.

A comparison of the zonal albedos of the Max product with the all-weather land albedo estimates of Kukla and Robinson (1980) shows the present product to have a wider zonal range. Compared to the 1980 figures, Max albedo is 0.05–0.10 higher in the polar regions and 0.05–0.15 lower between 55 and 70°. The 1980 values are based on the assignment of parameterized albedo estimates to the three visually derived brightness categories formerly plotted in the NOAA operational snow charts (Smigielski, 1981). The 1980 product was not meant to represent maximum conditions but can be assumed to be at or close to the maximum level north of 50°N.

TABLE 2. Zonal averages of surface albedo of Northern Hemisphere lands under maximum snow cover.*

Latitude (°)	Eurasia	North America	Northern Hemisphere
85–80	0.80	0.74	0.75
80–75	0.80	0.77	0.75
75–70	0.76	0.79	0.77
70–65	0.61	0.67	0.63
65–60	0.36	0.58	0.43
60–55	0.43	0.49	0.45
55–50	0.56	0.47	0.53
50–45	0.67	0.49	0.61
45–40	0.67	0.59	0.64
40–35	0.70	0.57	0.66
35–30*	0.72	0.56	0.69
30–25*	0.68		0.68
		mean	
85–25*	0.60	0.56	0.59

* Includes land having greater than a 0% probability of 2.5 cm or deeper snow cover at the end of January or February, according to Dickson and Posey (1967) (cf. Fig. 1). Greenland is excluded from the results and would raise the hemispheric value by 0.007.

5. Conclusions

The present description of the albedo of snow-covered surfaces is the most detailed available on a hemispheric scale. Information on the spatial distribution of surface brightness over snow-covered land is useful in the operational charting of snow and cloud covers. The product may also be of use in assessing the distribution of biomass, since the winter albedo values provide an indication of vegetative density. Finally, the $1 \times 1°$ data set should find use in climate modeling efforts, particularly so in investigations of potential climate change. The major climatic impacts of increasing CO_2 and other greenhouse constituents and of "nuclear winter" are expected to take place in seasonally snow-covered regions, primarily due to the snow-ice/albedo feedback (Ramanathan *et al.*, 1979; Robock, 1984).

Acknowledgments. Thanks to J. Gavin, W. Donn and G. Jacoby for reading the manuscript. This research was supported by NSF Grant ATM80-01470 and ATM82-00863. This is LDGO contribution 3801.

REFERENCES

Atmospheric Environment Service, 1978–84: *Climatic Perspectives,* Canadian Climate Centre.

Barnes, J. C., and C. J. Bowley, 1968: Snow cover distribution as mapped from satellite photography. *Water Resour. Res.,* **4,** 257–272.

——, and ——, 1977: Study of near-infrared snow reflectance using Skylab S192 multispectral scanner data. Environmental Research and Technology, Inc., Document, 1474F, 48 pp.

Bauer, K. G., and J. A. Dutton, 1962: Albedo variations measured from an airplane over several types of surface. *J. Geophys. Res.,* **67,** 2367–2376.

Bryazgin, N. N., and A. P. Koptev, 1970: Spectral albedo of snow-ice cover. *Prob. Arctic Antarctic,* **31,** 79–83.

Bunting, J. T., and R. P. d'Entremont, 1982: Improved cloud detection utilizing Defense Meteorological Satellite Program near infrared measurements. *Air Force Geophysics Laboratory* Env. Res. Pap. 765, 91 pp.

Carroll, J. J., and B. W. Fitch, 1981: Effects of solar elevation and cloudiness on snow albedo at the South Pole. *J. Geophys. Res.,* **86,** 5271–5276.

Conover, J. H., 1965: Note on the flora and snow cover distributions affecting the appearance of northeastern United States as photographed by TIROS satellites. *Mon. Wea. Rev.,* **93,** 644–646.

Dave, J. V., and R. Bernstein, 1982: Effect of terrain orientation and solar position on satellite-level luminance observations. *Rem. Sens. Environ.,* **12,** 331–348.

Dickson, R. R., and J. Posey, 1967: Maps of snow-cover probability for the Northern Hemisphere. *Mon. Wea. Rev.,* **95,** 347–353.

Dozier, J., and J. Frew, 1981: Atmospheric corrections to satellite radiometric data over rugged terrain. *Rem. Sens. Environ.,* **11,** 191–205.

Federer, C. A., 1968: Spatial variation of net radiation, albedo and surface temperature of forests. *J. Appl. Meteor.,* **7,** 789–795.

Fett, R. W., and W. A. Bohan, 1977: Navy tactical applications guide, techniques and applications of image analysis. NAVENVPREDRSCHFAC Appl. Rep. 77-03, Vol. 1, Section 1, 53 pp.

——, and R. G. Isaacs, 1979: Concerning causes of "anomalous gray shades" in DMSP visible imagery. *J. Appl. Meteor.,* **18,** 1340–1351.

Ginsburg, N., H. Fullard and H. C. Darby, Eds., 1970: *Aldine University Atlas.* Aldine, 208 pp.

Goodison, B., 1981: Compatibility of Canadian snowfall and snow cover data. *Water Resour. Res.,,* **17,** 893–900.

Grenfell, T. C., and G. A. Maykut, 1977: The optical properties of ice and snow in the Arctic basin. *J. Glaciol.,* **18,** 445–463.

Grenfell, T. C., D. K. Perovich and J. A. Ogren, 1981: Spectral albedos of an alpine snowpack. *Cold Regions Sci. and Technol.,* **4,** 121–127.

Gurney, R. J., and D. K. Hall, 1983: Satellite-derived surface energy balance estimates in the Alaskan sub-arctic. *J. Climate Appl. Meteor.,* **22,** 115–125.

Henderson-Sellers, A., 1980: Albedo changes-surface surveillance from satellites. *Clim. Change,* **2,** 275–281.

Hummel, J. R., and R. A. Reck, 1979: A global surface albedo model. *J. Appl. Meteor.,* **18,** 239–253.

Jackson, C. I., 1961: Estimates of total radiation and albedo in sub-arctic Canada. *Arch. Met. Geoph. Biokl.* **B10,** 193–199.

Jurik, T. W., and D. M. Gates, 1983: Albedo following fire in a northern hardwood forest. *J. Climate Appl. Meteor.,* **22,** 1733–1737.

Kondratyev, K. Ya., L. N. Dyachenko and M. P. Piatovskaya, 1974: On the relationship between the earth–atmosphere system albedo and the earth's surface albedo. *Earth Survey Problems,* Akademie-Verlag Berlin, 473–482.

——, V. I. Korzov, V. V. Mukhenberg and L. N. Dyachenko, 1982: The shortwave albedo and the surface emissivity. *Land Surface Processes in Atmospheric General Circulation Models,* P. S. Eagleson, Ed, Cambridge University Press, 463–514.

Kopanev, I. D., 1976a: Variations in the duration of stable snow cover in the USSR. *Soviet Hydrol.—Selec. Pap.,* **15,** 270–275.

——, 1976b: Probability estimate of snow-cover depth distribution. *Soviet Hydrol.—Selec. Pap.,* **15,** 281–287.

——, 1978: *Sneznyi Pokrov na Territorii SSSR.* (Snow Cover in the USSR Territory). Gidrometeoizdat, 182 pp.

Kowalik, W. S., S. E. Marsh and R. J. P. Lyon, 1982: A relation between Landsat digital numbers, surface reflectance and the cosine of the solar zenith angle. *Rem. Sens. Environ.,* **12,** 39–55.

Kukla, G., and D. Robinson, 1980: Annual cycle of surface albedo. *Mon. Wea. Rev.,* **108,** 56–68.

——, and ——, 1981: Maximum snow area density digital product. *Snow Watch 1980, Glaciological Data, GD-11,* G. Kukla, A. Hecht and D. Wiesnet, Eds., World Data Center A for Glaciology, 135–138.

Kung, E. C., R. A. Bryson and D. H. Lenschow, 1964: Study of a continental surface albedo on the basis of flight measurements and structure of the earth's surface cover over North America. *Mon. Wea. Rev.,* **22,** 543–564.

Kurilova, Yu. V., P. A. Kolosov, L. K. Poplavskaya and Yu. S. Sokolov, 1976: Investigation of the dynamics of snow cover melting form meteorological-satellite data. *Soviet Hydrol.—Selec. Pap.,* **15,** 1–6.

Lillesand, T. M., D. E. Meisner, A. LaMois Downs and R. L. Deuell, 1982: Use of GOES and TIROS/NOAA satellite data for snow-cover mapping. *Photogram. Eng. Rem. Sens.,* **48,** 251–259.

McFadden, J. D., and R. A. Ragotzkie, 1967: Climatological significance of albedo in central Canada. *J. Geophys. Res.,* **72,** 1135–1143.

McGinnis, D. F. Jr., J. S. Pritchard and D. R. Wiesnet, 1975: Snow depth and snow extent using VHRR data from the NOAA-2 satellite. NOAA Tech. Memo. NESS 63, 10 pp.

Male, D. H., and R. J. Granger, 1981: Snow surface energy exchange. *Water Resour. Res.,* **17,** 609–627.

Maykut, G. A., and P. E. Church, 1973: Radiation climate of Barrow, Alaska,, 1962–66. *J. Appl. Meteor.,* **12,** 620–628.

Matthews, E., 1983: Global vegetation and land use: New high-resolution data bases for climate studies. *J. Climate Appl. Meteor.,* **22,** 474–487.

Mekler, Y., and J. H. Joseph, 1983: Direct determination of surface

albedos from satellite imagery. *J. Climate Appl. Meteor.*, **22,** 530–536.

Namias, J., 1962: Influences of abnormal surface heat sources and sinks on atmospheric behavior. *Proceedings International Symposium on Numerical Weather Prediction in Tokyo,* 615–627.

National Geographic Society, 1976: Portrait USA: The First Color Photomosaic of the 48 Continuous United States, (scale = 1: 4.56 m).

Ni, J., J. York and R. Cardwell, 1975: Mosaic of Landsat imagery of China and surrounding regions. Dept. of Geological Science, Cornell University, (scale = 1:6 m).

Norton, C. C., F. R. Mosher and B. Hinton, 1979: An investigation of surface albedo variations during the recent Sahel drought. *J. Appl. Meteor.*, **18,** 1252–1262.

Olson, J., and J. Watts, 1982: Major world ecosystem complexes. (scale = 1:30 m).

O'Neill, A. D. J., and D. M. Gray, 1973: Spatial and temporal variations of the albedo of prairie snowpack. *Role of Snow and Ice in Hydrology, Proc. Banff Symp.,* Banff, UNESCO/WMO/IAHS, Vol. 1, 176–186.

Pease, R. W., C. B. Jenner and J. E. Lewis Jr., 1980: The influences of land use and land cover on climate: An analysis of the Washington-Baltimore area that couples remote sensing with numerical simulation. USGS Prof. Pap. 1099-A, 39 pp.

Petzold, D. E., 1977: An estimation technique for snow surface albedo. *Clim. Bull.*, **21,** 1–11.

Posey, J., and P. Clapp, 1964: Global distribution of normal surface albedo. *Geofis. Int.*, 33–48.

Potter, J. G., 1965: Snow cover. *Climatological Studies* 3, Canada Dept. of Transportation, Meteorological Branch, 69 pp.

Preuss, H. J., and J. F. Geleyn, 1980: Surface albedos derived from satellite data and their impact on forecast models. *Arch. Met. Geoph. Biokl.*, **A29,** 345–356.

Ramanathan, V., M. S. Lian and R. D. Cess, 1979: Increased atmospheric CO_2: Zonal and seasonal estimates of the effect on the radiation energy balance and surface temperature. *J. Geophys. Res.*, **84,** 4949–4958.

Richardson, A. J., 1982: Relating Landsat digital count values to ground reflectance for optically thin atmospheric conditions. *Appl. Opt.*, **21,** 1457–1464.

Robinson, D. A., 1984: Anthropogenic impact on winter surface albedo. Doctoral thesis, Columbia University, 384 pp.

——, and G. Kukla, 1982: Remotely sensed characteristics of snow covered lands. *1982 International Geoscience and Remote Sensing Symposium Digest,* W. Keydel, Ed., IEEE, WA-1, 2.1–2.9.

—— and ——, 1984: Albedo of a dissipating snow cover. *J. Climate Appl. Meteor.*, **23,** 1626–1634.

——, M. Wilson, G. Kukla and A. Henderson-Sellers, 1983: Observation of surface albedo and its variation for climate models. Proceedings, *17th Int. Symp. Remote Sensing of Environment,* Ann Arbor, ERIM, 469–477.

Robock, A., 1980: The seasonal cycle of snow cover, sea ice and surface albedo. *Mon. Wea. Rev.*, **108,** 267–285.

——, 1984: Snow and ice feedbacks prolong effects of nuclear winter. *Nature,* **310,** 667–670.

Rockwood, A. A., and S. K. Cox, 1978: Satellite inferred surface albedo over Northwestern Africa. *J. Atmos. Sci.*, **35,** 513–522.

Shine, K. P., and A. Henderson-Sellers, 1983. Cryosphere-cloud interactions near the snow/ice limit: Sensitivity testing of model parameterizations. Final Rep. NSF Grant ATM 80-18898, University of Liverpool, 158 pp.

Shurov, S. I., Ed., 1954: *Atlas Mira.* Glavnoe Upravlenie Geodexii I Kartografii MVD SSSR, Moskva, 369 pp.

Smigielski, F., 1981: Northern Hemisphere snow and ice charts of NOAA/NESS. *Snow Watch 1980, Glaciological Data, GD-11,* G. Kukla, A. Hecht and D. Wiesnet, Eds., World Data Center A for Glaciology, 59–62.

Taylor, V. R., and L. L. Stowe, 1984: Reflectance characteristics of uniform earth and cloud surfaces derived from NIMBUS-7 ERB. *J. Geophys. Res.*, **89,** 4987–4996.

U.S. Dept. of Agriculture Soil Conservation Service, 1974: Conterminous United States: Mosaic of Imagery from Earth Resources Technology Satellite-1, USGS (scale = 1:5 m).

U.S. Dept. of Commerce, 1978–79: *Climatological Data,* National Oceanic and Atmospheric Administration, (monthly for various states and regions).

——, 1914– : *Weekly Weather and Crop Bulletin.,* National Oceanic and Atmospheric Administration.

Vukovich, F. M., 1983: An analysis of the ground temperature and reflectivity pattern about St. Louis, Missouri, using HCMM satellite data. *J. Climate Appl. Meteor.*, **22,** 560–571.

Wark, D. Q., R. W. Popham, W. A. Dotson and K. S. Colaw, 1962: Ice Observations by the TIROS II satellite and by aircraft. *Arctic,* **15,** 9–26.

Wiebecke, C., Ed., 1971: *Welt Forstatlas,* Paul Parey, Hamburg.

Woronicz, R. C., 1981: The U.S. Air Force snow cover charts. *Snow Watch 1980, Glaciological Data,* G. Kukla, A. Hecht and D. Wiesnet, Eds., GD-11, World Data Center A for Glaciology, 63–69.